Beamforming for Fully-Overlapped Two-Dimensional Phased-MIMO Radar

Anastasios Deligiannis, Sangarapillai Lambotharan
School of Electronic, Electrical and Systems Engineering
Loughborough University, Leicestershire, UK, LE11 3TU
Emails: {A.Deligiannis, S.Lambotharan}@lboro.ac.uk

Jonathon A. Chambers
Department of Electronic Engineering
University of Surrey, Guildford, UK, GU2 7XH
Email: j.a.chambers@surrey.ac.uk

***Abstract*—We investigate the design of joint transmitter and receiver beamformer within the context of multiple-input multiple-output (MIMO) radar employing two-dimensional (2D) arrays of antennas. Specifically, we derive the transmit, waveform diversity and overall transmit-receive beampatterns for the Phased-MIMO radar with fully-overlapped subarrays and compare them with the respective beampatterns for the Phased-array and MIMO radar only schemes. As reported for one-dimensional linear arrays, fully-overlapped 2D subarrays offer substantial improvements in performance as compared with the phased-array and MIMO only radar models. The work considers both the adaptive (convex optimization, CAPON beamformer) and non-adaptive (conventional) beamforming techniques. The simulation results demonstrate the superiority of the fully-overlapped subaperturing in both cases.**

I. Introduction

The field of radar research is vast and has been endlessly developing since late 1930's. The gigantic breakthroughs in digital signal processing and the constant growth in computational capabilities have enabled the introduction of an emerging technology known as multiple-input multiple-output (MIMO) radar [1]. The essence of MIMO radar is the use of multiple antennas to simultaneously transmit diverse, possibly linearly independent waveforms, in contrast to a phased-array radar which transmits scaled versions of a single waveform. This waveform diversity offers superior capabilities as compared to the phased-array model. There are two fundamental regimes of operation investigated in the literature. In the first type, the transmit and receive antenna elements are widely spaced, whereas, in the second type, the antenna elements are closely spaced.

MIMO radar with colocated antennas [2] is known to offer higher sensitivity to detect slowly moving targets, higher angular resolution, increased number of detectable targets, direct applicability of adaptive array techniques and better parameter identifiability. On the other hand, MIMO radar with widely spaced antennas provides the ability to capture the spatial diversity of the target's radar cross section (RCS), enhance the ability to combat signal scintillation, estimate precisely the parameters of fast moving targets and improve the target detection performance, by taking advantage of the target's geometrical characteristics [3].

The substantial improvements offered by MIMO radar technology come at the cost of losing the transmit coherent processing gain offered by phased-array radar [4], [6]. This absence can lead to signal-to-noise ratio (SNR) decrease and beam-shape loss [4], [6]. The aforementioned disadvantages raise the dilemma of whether or not MIMO radar will meet the expectations that it will provide a colossal opportunity for improvements in the field of radar research. This work stems from the belief that MIMO radar is not a substitute technology that will totally outclass phased-array radars, but rather it provides the opportunity of jointly exploiting the benefits of both models, as reported recently in the literature [6], [8]. The authors of [8] proposed a radar model, utilizing the idea of dividing a large number of colocated transmit/receive elements into multiple subarrays, that are not allowed to overlap. Phased-MIMO radar is a breakthrough notion in radar technology, introduced in [6]. The vantage point of this technique is the partition of the transmit array into subarrays that are allowed to overlap. Our earlier work in [7] investigated the application of this Phased-MIMO radar notion to 2D transmit arrays by designing the transmit beampattern through a convex optimization problem that minimizes the difference between a desired transmit beampattern and the actual one produced by the system [1].

In this paper, we examine transmit, waveform diversity and overall transmit-receive beamforming design for Phased-MIMO radar with fully-overlapped 2D transmit subarrays. We design the Phased-MIMO beampatterns using both conventional and adaptive techniques and compare them with the respective beampatterns of the phased-array and MIMO radars. Specifically, in order to design the adaptive transmit beampattern, we solve a convex optimization problem that minimizes the difference between a desired transmit beampattern and the actual one produced by the system. Furthermore, we obtain the adaptive overall transmit-receive beampattern by utilizing the Minimum Variance Distortionless Response (MVDR) Capon beamformer. The simulation results highlight the benefits provided by the 2D Phased-MIMO radar with fully overlapped subarrays.

II. 2D Phased-MIMO System Model

We consider a monostatic radar system employing a uniform rectangular array (URA), which consist of $M_t \times N_t$ and $M_r \times N_r$ antennas at the transmitter and the receiver respectfully, where M_t and M_r are the number of elements

978-1-4799-8232-5/151$31.00@2015IEEE

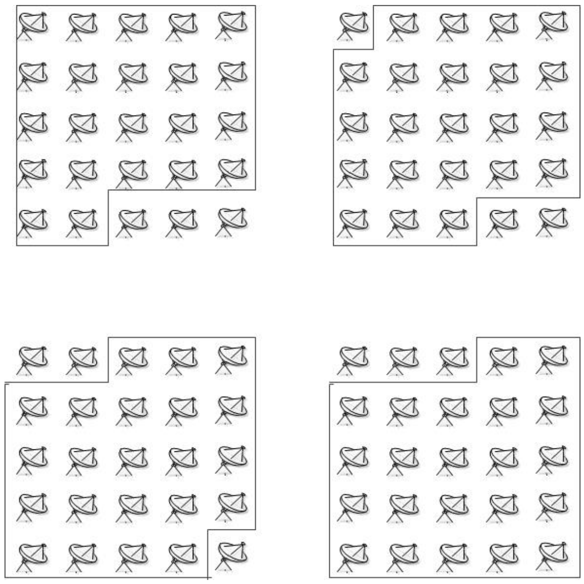

Fig. 1: Fully overlapped subaperturing of a 5×5 uniform rectangular array (URA) when K=4.

in each column and N_t and N_r are the number of antennas in each row of the planar arrays. The 2D Phased-MIMO model is based on partitioning the transmit 2D array into K subarrays ($1 \leq K \leq M_t \times N_t$) that are fully overlapped [6], as depicted in Fig.1, where a subaperturing of a 5×5 transmit URA into 4 subarrays is presented. Moreover the k^{th} subarray is composed of $M_t \times N_t - K + 1$ antennas and emits the k^{th} element of the predesigned independent waveform vector $\boldsymbol{\psi}(t) = [\psi_1(t), \ldots, \psi_K(t)]^T$ of size $K \times 1$, which satisfies the orthogonality condition $\int_{T_0} \boldsymbol{\psi}(t)\boldsymbol{\psi}^H(t)dt = \mathbf{I}_K$, where $(\cdot)^T$ denotes the transpose, t refers to the time index within the radar pulse, T_0 is the radar pulse width, $\mathbf{I}_K$ is the $K \times K$ identity matrix, and $(\cdot)^H$ denotes the Hermitian transpose.

In order to characterize the fully overlapped subaperturing of the 2D Phased-MIMO model mathematically, we introduce an $M_t \times N_t$ selection matrix $\mathbf{Z}_k$ [5]. When the $(mn)^{th}$ entry equals 1 then the $(mn)^{th}$ element of the 2D array belongs to the k^{th} subarray, while a 0 entry in $\mathbf{Z}_k$ means that the element is not a part of the k^{th} subarray. Thus, the matrix $\mathbf{Z}_k$ defines the structure of the k^{th} subarray. As a result, the $M_tN_t \times 1$ transmit steering vector related to the k^{th} subarray can be constructed as:

$$\mathbf{a}_k(\theta, \phi) = vec(\mathbf{Z}_k \odot [\boldsymbol{\mu}(\theta, \phi)\boldsymbol{\nu}^T(\theta, \phi)]) \tag{1}$$

where $vec(\cdot)$ is the operator that stacks the columns of a matrix into one column vector, $\odot$ denotes the Hadamard product, θ and ϕ denote the elevation and azimuth angles respectively. The auxiliary vectors $\boldsymbol{\mu}(\theta, \phi) \in C^{M_t \times 1}$ and $\boldsymbol{\nu}(\theta, \phi) \in C^{N_t \times 1}$ are derived from the array geometry and they are defined as follows:

$$\boldsymbol{\mu}(\theta, \phi) = [1, e^{j2\pi d_m sin(\theta)cos(\phi)}, \ldots, e^{j2\pi(M_t-1)d_m sin(\theta)cos(\phi)}]^T$$

$$\boldsymbol{\nu}(\theta, \phi) = [1, e^{j2\pi d_n sin(\theta)sin(\phi)}, \ldots, e^{j2\pi(N_t-1)d_n sin(\theta)sin(\phi)}]^T$$

where d_m and d_n are the distances between the adjacent antennas at each column and at each row respectively.

Our primary objective is to focus the transmit energy onto a certain 2D sector in space, determined by the direction of the target, and at the same time to achieve high transmit coherent processing gain. Hence, a weight vector should be designed for each of the K subarrays to steer the transmit beam in the desired spatial sector. The $M_tN_t \times 1$ vector which consists of the complex envelope of the signals at the output of the k^{th} subarray can be modeled as $\mathbf{s}_k(t) = \sqrt{\frac{M_tN_t}{K}}\mathbf{w}_k\psi_k(t)$, where $\mathbf{w}_k \in C^{M_tN_t \times 1}$ is the transmit beamformer weight vector, used to form the k^{th} transmit beam. The power of the emitted signal from the k^{th} subarray focused at a generic focal point with coordinates (θ, ϕ) is given by

$$P_k(\theta, \phi) = \mathbf{a}_k^H(\theta, \phi)E\{\mathbf{s}_k(t)\mathbf{s}_k^H(t)\}\mathbf{a}_k(\theta, \phi)$$

$$= \frac{M_tN_t}{K}\mathbf{a}_k^H(\theta, \phi)\mathbf{w}_k\mathbf{w}_k^H\mathbf{a}_k(\theta, \phi) \tag{2}$$

Using the far field assumption and adding the power of the probing signals emitted by all K subarrays, we write the 2D array transmit beampattern as

$$P(\theta, \phi) = \sum_{k=1}^{K} \frac{M_tN_t}{K}\mathbf{a}_k^H(\theta, \phi)\mathbf{w}_k\mathbf{w}_k^H\mathbf{a}_k(\theta, \phi) \tag{3}$$

Assuming that there is a target present in the far-field of the transmit and receive arrays at direction θ_t in the elevation domain and ϕ_t in the azimuth domain, the signal reflected by the aforementioned target is modeled as

$$r(t, \theta_t, \phi_t) = \sqrt{\frac{M_tN_t}{K}}\beta_t \sum_{k=1}^{K} \mathbf{w}_k^H\mathbf{a}_k(\theta_t, \phi_t)e^{-j\tau_k(\theta_t, \phi_t)}\psi_k(t) \tag{4}$$

where β_t is the complex amplitude proportional to the radar cross section (RCS) of the target, and $\tau_k(\theta_t, \phi_t)$ is the time required for the signal to cover the distance between the first element of the transmit array and the first element of the k^{th} subarray.

If we assume that in addition to the desired target, there are L active interfering targets at locations $\{\theta_i\}_{i=1}^L$, $\{\phi_i\}_{i=1}^L$ and with reflection coefficients $\{\beta_i\}_{i=1}^L$, then under the simplifying assumption of point targets, the $M_rN_r \times 1$ received data vector can be described by the equation

$$\mathbf{x}(t) = r(t, \theta_t, \phi_t)\mathbf{b}(\theta_t, \phi_t) + \sum_{i=1}^{L} r(t, \theta_i, \phi_i)\mathbf{b}(\theta_i, \phi_i) + \mathbf{n}(t) \tag{5}$$

where $\mathbf{b}(\theta, \phi)$ is the $M_rN_r \times 1$ steering vector of the received array and $\mathbf{n}(t)$ is the noise component that is supposed to have zero mean. By applying matched filtering to the received data vector for each of the orthogonal waveforms $\psi_k(t)$, $k =$

$1, ..., K$, we can construct the $KM_rN_r \times 1$ virtual receive data vector as

$$\mathbf{y} = \int_{T_0} \mathbf{x}(t)\psi_k^*(t)dt$$

$$= \sqrt{\frac{M_tN_t}{K}}\beta_t\mathbf{u}(\theta_t, \phi_t) + \sum_{i=1}^{L}\sqrt{\frac{M_tN_t}{K}}\beta_i\mathbf{u}(\theta_i, \phi_i) + \hat{\mathbf{n}} \quad (6)$$

where $\hat{\mathbf{n}} = \int_{T_0} \mathbf{n}(t)\psi_k^*(t)dt$ is the $KM_rN_r \times 1$ noise term with covariance matrix $\mathbf{R}_n = \sigma_n^2\mathbf{I}_{KM_rN_r}$ (σ_n^2 is the noise variance) and the $KM_rN_r \times 1$ vector

$$\mathbf{u}(\theta, \phi) = (\mathbf{c}(\theta, \phi) \odot \mathbf{d}(\theta, \phi)) \otimes \mathbf{b}(\theta, \phi) \quad (7)$$

is the virtual steering vector of the system. In order to derive the virtual steering vector we used the $K \times 1$ transmit coherent processing vector

$$\mathbf{c}(\theta, \phi) = [\mathbf{w}_1^H\mathbf{a}_1(\theta, \phi), \ldots, \mathbf{w}_K^H\mathbf{a}_K(\theta, \phi)]^T \quad (8)$$

and the $K \times 1$ waveform diversity vector

$$\mathbf{d}(\theta, \phi) = [e^{-j\tau_1(\theta,\phi)}, \ldots, e^{-j\tau_K(\theta,\phi)}]^T \quad (9)$$

In the case of the fully-overlapped partitioning of the 2D transmit array into K subarrays, the waveform diversity vector is equal to the K first elements of the transmit steering vector $\mathbf{a}(\theta, \phi) = vec(\boldsymbol{\mu}(\theta, \phi)\boldsymbol{\nu}^T(\theta, \phi))$.

At this point it is apparent that the 2D Phased-MIMO radar scheme exploits the benefits of both the phased-array and the MIMO radar model as a tradeoff between transmit coherent processing gain and higher angular resolution. This tradeoff is determined by the selection of the number of fully overlapped subarrays of the 2D transmit array. In particular, if we choose $K = 1$ the radar model simplifies to the conventional phased-array scheme, since the whole transmit array forms the only subarray which emits only one waveform. However, if $K = M_tN_t$ is selected, the radar model simplifies to a MIMO radar.

III. TRANSMIT-RECEIVE BEAMFORMING FOR THE PHASED-MIMO MODEL

In this section, we investigate conventional and adaptive techniques to design the transmit and the overall transmit-receive beampattern of the Phased-array, Phased-MIMO and MIMO radar schemes.

A. Conventional Beampattern Design

Conventional non-adaptive beamforming is the simplest technique to design the transmit and overall beampatterns, however, it offers the highest possible output SNR gain only when a single target is observed in the background of white Gaussian noise [9]. By applying the conventional beamforming in the proposed 2D Phased-MIMO model, the normalized transmit weight vector for the k^{th} subarray can be obtained as

$$\mathbf{w}_k = \frac{\mathbf{a}_k(\theta_t, \phi_t)}{\|\mathbf{a}_k(\theta_t, \phi_t)\|}, \quad k = 1, \ldots, K \quad (10)$$

where $|| \cdot ||$ denotes the Euclidian norm. In order to derive the conventional transmit beampattern, we substitute (10) in (3). By enforcing the conventional beamformer at the virtual receive array, the $KM_rN_r \times 1$ receive weight vector is defined as

$$\mathbf{w}_r = \mathbf{u}(\theta_t, \phi_t) \quad (11)$$

As a result, the overall transmit-receive beampattern is given by

$$Q(\theta, \phi) = |\mathbf{w}_r^H\mathbf{u}(\theta, \phi)|^2 \quad (12)$$

B. Adaptive Beampattern Design

After we obtain the target location coordinates from the detection scan of the radar system as (θ_t,ϕ_t), our main goal is to focus the power of the next beam at a spatial sector around the target, defined by

$$\Theta = [\theta_t - \Delta_1, \quad \theta_t + \Delta_1] \quad (13)$$

$$\Phi = [\phi_t - \Delta_2, \quad \phi_t + \Delta_2] \quad (14)$$

in the elevation domain and the azimuth domain, where $2\Delta_1$ and $2\Delta_2$ are the chosen beamwidths for the target in the elevation and azimuth domain respectively (Δ_1 and Δ_2 should be greater than the expected error in θ_t and ϕ_t respectively). Following this approach, we obtain more accurate parameter identifiability for the target. The derivation of the transmit weight vector for each subarray is achieved by solving a convex optimization problem that minimizes the difference between the desired transmit beampattern and the beampattern produced by the 2D array of antennas, under a constraint in terms of uniform power allocation across the transmit antennas [5], [7]. In this work, we consider strong clutter imposed by an obstacle within a certain 2D spatial sector, already estimated as $\Theta_c = [\theta_{c1} \quad \theta_{c2}]$ and $\Phi_c = [\phi_{c1} \quad \phi_{c2}]$ from training signals. The second constraint in our optimization problem is to restrain the sidelobe level in the prescribed region under a certain value δ, thus minimizing the clutter effect in our system. Hence, defining a matrix $\mathbf{X}_k = \mathbf{w}_k\mathbf{w}_k^H \in C^{M_tN_t \times M_tN_t}, k = 1, ..., K$, we formulate the optimization problem as:

$$\min_{\mathbf{X}_1,\ldots,\mathbf{X}_K} \quad \max_{\theta,\phi} |P_d(\theta, \phi) - \sum_{k=1}^{K} Tr\{\mathbf{a}_k(\theta, \phi)\mathbf{a}_k^H(\theta, \phi)\mathbf{X}_k\}|$$

$$s.t. \quad \sum_{k=1}^{K} diag\{\mathbf{X}_k\} = \frac{E}{M_tN_t - (K-1)}\mathbf{1}_{M_tN_t \times 1}$$

$$|\sum_{k=1}^{K} Tr\{\mathbf{a}_k(\theta_c, \phi_c)\mathbf{a}_k^H(\theta_c, \phi_c)\mathbf{X}_k\}| - \delta \leq 0, \quad \theta_c \in \Theta_c, \phi_c \in \Phi_c$$

$$\mathbf{X}_k \succeq 0, \quad k = 1, \ldots, K \quad (15)$$

where $P_d(\theta, \phi)$ is the desired beampattern, E is the total available power, $Tr\{\cdot\}$ denotes the trace of a matrix, $diag\{\cdot\}$

denotes the diagonal of a square matrix and $\mathbf{1}_{M_t N_t}$ defines the $M_t N_t \times 1$ vector of ones. We use $\mathbf{X}_k \succeq 0, \quad k = 1, \ldots, K$ to indicate that $\mathbf{X}_k$ is positive semidefinite. The convex optimization problem (15) is solved using semidefinite programming (SDP) [10]. After obtaining the optimal solution, denoted as $\mathbf{X}_k^*$, we derive the optimal transmit weight vectors $\mathbf{w}_k$. If $\mathbf{X}_k^*$ is of rank one, which is the ideal scenario, the optimal weight vector $\mathbf{w}_k$ is obtained straightforwardly as the principal eigenvector of $\mathbf{X}_k^*$ multiplied by the square root of the principal eigenvalue of $\mathbf{X}_k^*$. However, if the rank of $\mathbf{X}_k^*$ is greater than one, we resort to randomization techniques to obtain the optimal transmit weight vectors [7].

Besides the transmit array, it is also important to use adaptive techniques at the 2D receive array of the system in order to maximize the output signal to interference plus noise ratio (SINR). A beamformer that satisfies both the steering capabilities whereby the target signal is always protected and the cancellation of interference so that the output SINR is maximized, is the Minimum Variance Distortionless Response (MVDR) beamformer [11]. The main idea of the MVDR beamformer is to minimize the covariance of the beamformer output subject to a distortionless response towards the direction of the target. Hence, it can be formulated as the following optimization problem

$$\min_{\mathbf{w}_r} \mathbf{w_r^H} \hat{\mathbf{R}}_{yy} \mathbf{w_r} \quad \text{subject to} \quad \mathbf{w_r^H} \mathbf{u}(\theta_t, \phi_t) = 1 \tag{16}$$

where $\hat{\mathbf{R}}_{yy} = \frac{1}{N} \mathbf{y}\mathbf{y}^H$ is the sample covariance matrix of the observed data samples that can be collected from N different radar pulses. The solution to (16) is [11],

$$\mathbf{w_r} = \frac{\hat{\mathbf{R}}_{yy}^{-1} \mathbf{u}(\theta_t, \phi_t)}{\mathbf{u}^H(\theta_t, \phi_t) \hat{\mathbf{R}}_{yy}^{-1} \mathbf{u}(\theta_t, \phi_t)} \tag{17}$$

The receive weight vectors derived by (17) are employed to design the overall transmit-receive beampattern in our simulations.

IV. Simulation Results

We compare the performance of the fully-overlapped 2D Phased-MIMO radar to the phased-array and the conventional MIMO radar schemes. We assume a 5×5 transmit-receive URA with half-wavelength spacing between adjoining antennas ($d_m = d_n = \lambda/2$, where λ is the wavelength). The emitted orthogonal baseband waveforms from each subarray are modeled as [12]:

$$\psi_k(t) = \sqrt{\frac{1}{T_0}} e^{j2\pi(k/T_0)t}, \quad k = 1, \ldots, K$$

The target we wish to detect is located at directions $\theta_t = -30^o$ and $\phi_t = 60^o$. Furthermore, we assume one interfering target at directions $\theta_i = 30^o$ and $\phi_i = 90^o$. The 2D transmit array is divided into 5 subarrays that are fully overlapped and each of them consists of 21 antennas. The noise is considered as complex Gaussian with zero mean and variance 0.1. In order to derive the sample covariance matrix we use $N = 100$ data samples.

In the first example, we use the conventional non-adaptive beamformer to derive both the transmit and receive weight vectors. In order to obtain the waveform diversity beampattern, we consider the waveform diversity vector obtained by (9) as the weight vector. As a result, the transmit, the waveform diversity and the overall beampatterns for the 2D Phased-MIMO radar are depicted in Fig. 2. In Fig. 3, we simulate the same beampatterns for the phased-array radar model, by considering the whole 2D transmit array as the only subarray ($K = 1$). On the contrary, in order to simulate the conventional MIMO radar, we set $K = M_t N_t$ (each antenna of the transmit array is considered as a subarray) and the respective beampatterns are shown in Fig. 4. To facilitate the comparison between the three models, Figs. 5-7 show the cross section plotted against the elevation angle by keeping the azimuth angle constant at 60^o as well as the cross section plotted against the azimuth angle by holding the elevation angle at -30^o for all three schemes.

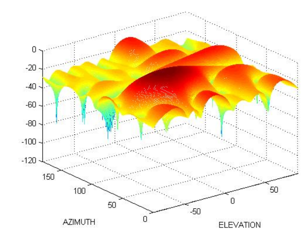

(a) Conventional transmit beampattern (dB).

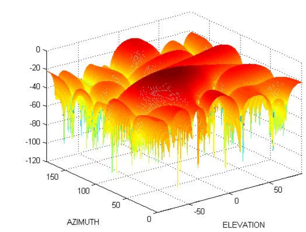

(b) Conventional waveform diversity beampattern (dB).

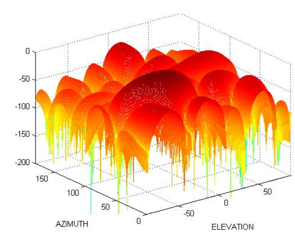

(c) Conventional overall beampattern (dB).

Fig. 2: The beampatterns for the non-adaptive 2D Phased-MIMO radar.

As reported for the case of the one-dimensional (1D) linear array in [6], for the 2D array also it is evident from Figs. 5 and 6 that although the phased-array radar has the most efficient transmit conventional beampattern due to its high transmit coherent processing gain, it has zero waveform diversity gain. On the other hand, the MIMO radar has flat ($0dB$) transmit beampattern, but it has the most accurate waveform diversity beampattern, because of the simultaneous emission of $M_t N_t$ orthogonal waveforms. However, it is clear from Fig. 7 that the 2D Phased-MIMO radar remarkably outperforms the phased-array and MIMO radars in terms of the overall transmit-receive beampattern, as it has lower sidelobes and approximates better

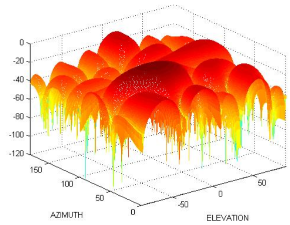

(a) Conventional transmit beampattern (dB).

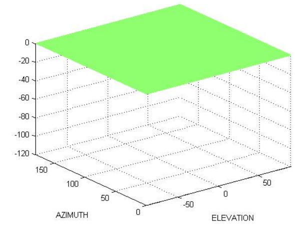

(b) Conventional waveform diversity beampattern (dB).

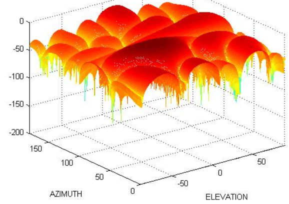

(c) Conventional overall beampattern (dB).

Fig. 3: The beampatterns for the non-adaptive 2D phased-array radar.

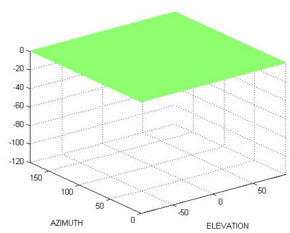

(a) Conventional transmit beampattern (dB).

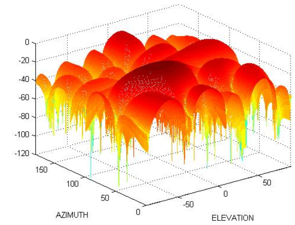

(b) Conventional waveform diversity beampattern (dB).

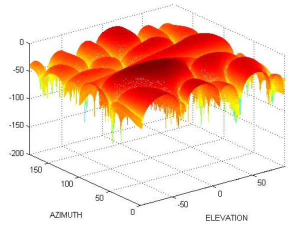

(c) Conventional overall beampattern (dB).

Fig. 4: The beampatterns for the non-adaptive 2D MIMO radar.

the desired target direction. Moreover, it is important to highlight that in the case of conventional beamforming the overall beampatterns of the phased-array and the MIMO radar are exactly the same.

In the second example, we employ adaptive beamforming techniques to derive the transmit and receive beampatterns. In particular, we use convex optimization techniques to determine the transmit beamformer weight vectors and the MVDR (CAPON) based receiver beamformer for the receive

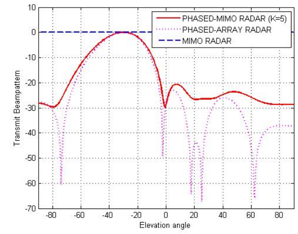

(a) Elevation cross section.

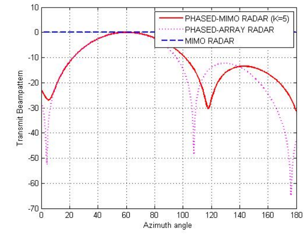

(b) Azimuth cross section.

Fig. 5: Cross sections of the transmit beampattern at $\phi = 60^o$ and $\theta = -30^o$, respectively.

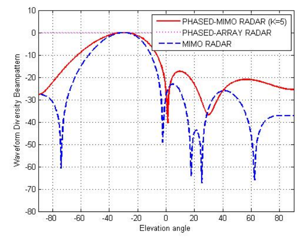

(a) Elevation cross section.

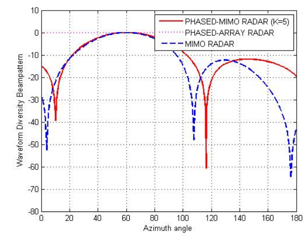

(b) Azimuth cross section.

Fig. 6: Cross sections of the waveform diversity beampattern at $\phi = 60^o$ and $\theta = -30^o$, respectively.

weight vectors. In our simulations we assume strong clutter at the 2D spatial sector defined by $\Theta_c = [-90^o, -60^o]$ and $\Phi_c = [140^o, 180^o]$. We consider $\delta = 0.01$ (-20dB) to restrain the sidelobe level in the clutter region. The desired beampattern that we wish to approximate is given by (13) and (14) where we set $\Delta_1 = 10^o$ and $\Delta_2 = 20^o$. The total available power for our system is equal to one ($E = 1$) and the interference to noise ratio (INR) is fixed to 30dB. The 2D transmit beampattern for the Phased-MIMO radar is obtained by solving the optimization problem in (15) as shown in Fig. 8a. Similarly, by solving the same optimization problem considering the whole URA as one subarray ($K = 1$), we generated the 2D transmit beampattern for the phased-array scheme as shown in Fig. 8b. It is clear that the power allocation of both beampatterns is concentrated in the desired space and the sidelobe level is very low, especially over the predefined

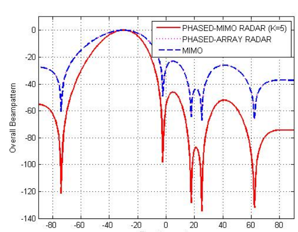

(a) Elevation cross section.

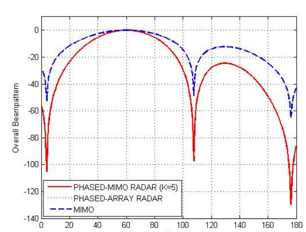

(b) Azimuth cross section.

Fig. 7: Cross sections of the overall beampattern at $\phi = 60^o$ and $\theta = -30^o$, respectively.

clutter regions, where it has values lower than 20dB.

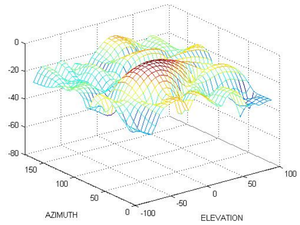

(a) 2D Phased-MIMO radar.

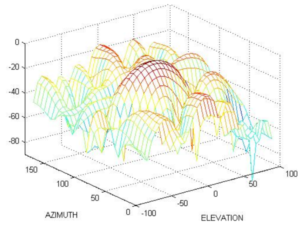

(b) 2D Phased-array radar.

Fig. 8: Transmit beampatterns using convex optimization(dB).

At the receive array, the MVDR beamformer is employed to derive the overall transmit-receive beampatterns for all radar schemes investigated, as shown in Fig. 9. Similar to the first example, Fig. 10 shows the cross sections of the overall beampatterns to help us facilitate the comparison between the three types of radar configurations. Corresponding to the results for conventional beamforming, it is clear from Fig. 10 that the 2D Phased-MIMO radar exploits the transmit superiority of the phased-array model and the waveform diversity of the MIMO scheme to result in a substantially improved overall beampattern.

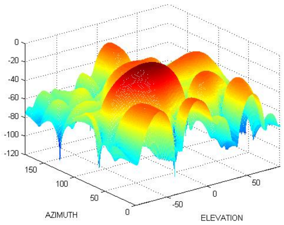

(a) 2D Phased-MIMO radar.

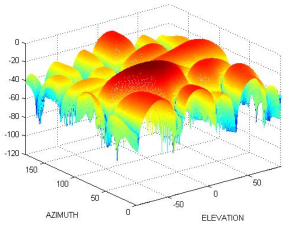

(b) 2D phased-array radar.

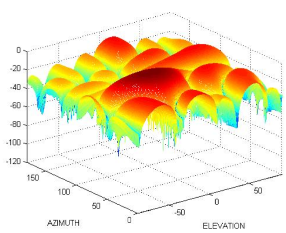

(c) 2D MIMO radar.

Fig. 9: Adaptive Overall Beampatterns using MVDR beamformer (dB).

V. Conclusion

We have investigated the performance of transmit/receive beamforming within the context of 2D Phased-MIMO radar with fully overlapped subarrays. The simulation results confirmed that there are substantial improvements of the overall transmit/receive beampattern of the 2D Phased-MIMO radar as compared to the phased-array and the conventional MIMO

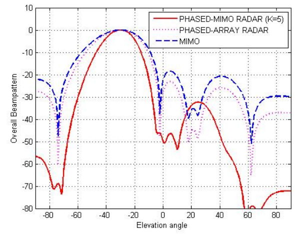

(a) Elevation cross section.

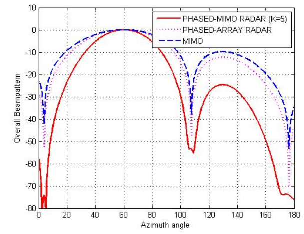

(b) Azimuth cross section.

Fig. 10: Cross sections of the overall beampattern at $\phi = 60^o$ and $\theta = -30^o$ (adaptive beamforming).

model. In particular, it was demonstrated that the Phased-MIMO scheme combines the transmit coherent processing gain of the phased-array radar and the waveform diversity of the MIMO model to produce a more efficient and accurate overall beampattern with very low sidelobe levels. This superiority is highlighted using both non-adaptive (conventional) and adaptive (convex optimization and MVDR) beamforming techniques.

Acknowledgment

This work was supported by the Engineering and Physical Sciences Research Council (EPSRC) Grant number EP/K014307/1 and the MOD University Defence Research Collaboration (UDRC) in Signal Processing.

References

[1] J. Li, and P. Stoica, *"MIMO Radar Signal Processing"*. New Jersey: WILEY, 2009.

[2] J. Li, and P. Stoica, *"MIMO Radar with Colocated Antennas"*. IEEE Signal Processing Magazine, **24**(5):106-114, Sep. 2007.

[3] A. M. Haimovich, R. S. Blum, and L. J. Cimini, *"MIMO Radar with Widely Separated Antennas"*. IEEE Signal Processing Magazine, **25**(1):116-129, Jan. 2008.

[4] F. Daum, and J. Huang, *"MIMO radar: snake oil or good idea?"*. IEEE Aerosp. Electron. Syst. Magazine, pp.8-12, **25**(1):116-129, May 2009.

[5] A. Hassanien, M. W. Morency, A. Khabbazibasmenj, S. A. Vorobyov, J.-Y. Park, and S.-J. Kim *"Two-Dimensional Transmit Beamforming for MIMO Radar with Sparse Symmetric Arrays"*. IEEE Radar Conference (RADAR), pp.1-6, Ottawa, ON, May 2013.

[6] A. Hassanien, and S. A. Vorobyov, *"Phased-MIMO Radar: A Tradeoff Between Phased-Array and MIMO Radars"*. IEEE Trans. Signal Processing, **58**(6):3137-3151, Jun. 2010.

[7] A. Deligiannis, J. A. Chambers, and S. Lambotharan, *"Transmit Beamforming Design for Two-Dimensional Phased-MIMO Radar with Fully-Overlapped Subarrays"*, Sensor Signal Processing for Defence (SSPD), Edinburgh, Sep. 2014.

[8] D. R. Fuhrmann, J. P. Browning, and M. Rangaswamy, *"Signaling Strategies for the Hybrid MIMO Phased-Array Radar"*. IEEE Journal, Selected Topics in Signal Processing, **4**(1):66-78, Feb. 2010.

[9] H. L. Van Trees, *"Optimum Array Processing"*. New York: WILEY, 2002.

[10] S. Boyd and L. Vandenberghe, *"Convex Optimization"*. Cambridge University Press, 2004.

[11] P. Stoica and R. L. Moses, *"Spectral Analysis of Signals"*. Prentice-Hall, Upper Saddle River, NJ, 2005.

[12] Q. He, R. Blum, and A. Haimovich, *"Target Velocity Estimation and Antenna Placement for MIMO Radar With Widely Separated Antennas"*. IEEE Journal, Selected Topics in Signal Processing, **4**(1):79-100, Feb. 2010.